

# Observing Elliptical Galaxies with the IPCS

M.-H. Ulrich, ESO Scientific Group, Geneva

## 1. Introduction

The Image Photon Counting System (IPCS) developed in the early 1970's at University College London by Dr. A. Boksenberg and collaborators (A. Boksenberg, 1972 in *Auxiliary Instrumentation for Large Telescopes*, proceedings of ESO/CERN Conference, p. 295; A. Boksenberg and D. E. Burgess, 1972 in *Adv. in Electronics and Electron Physics*, 33B p. 285) is a two-dimensional detector. It has been used on the ESO 3.6-m telescope at La Silla to observe spectrographically a variety of faint astronomical objects: extended objects, in particular regions of galaxies outside the nucleus, nebulosities associated with active nuclei, etc., and star-like objects such as quasars or halo stars.

In this article we report on observations made with this detector attached to the Boller and Chivens spectrograph of the 3.6-m telescope.

The detector is described in section 2. The data acquisition and data reduction are outlined in section 3. Results on elliptical galaxies are presented in section 4.

## 2. Description of the UCL Image Photon Counting System (IPCS)

The conceptual design of the system is based on

- (1) a combination of an image intensifier and a television camera tube having sufficient over-all gain to enable the photon events to be recorded easily and unequivocally;
- (2) the electronic processing and storage functions which were especially developed to analyse and record each photon event individually. System noise and ion events are eliminated, and a pattern recognition logic analyses the spread of each scintillation, resulting in a substantial increase in resolution over that obtained by conventional analogue integration. The position of each centroided photon event is transferred to a small on-line computer where the appropriate memory addresses are incremented.

The system is photoelectron noise limited and its efficiency is essentially the quantum efficiency of the first photocathode of the image intensifier. Storage capacity depends only on the size of the on-line computer memory and is therefore effectively unlimited.

These characteristics make this instrument particularly well suited to observations of faint astronomical objects.

One of the first versions of the IPCS built by Boksenberg was carried to various observatories and installed on large telescopes for periods of a few days to a few weeks. Boksenberg has extensively and successfully used it at Hale Observatories, KPNO, and the RGO, usually in collaboration with local astronomers. Other copies of the IPCS, with some minor modifications, have recently been built and are in operation at the AAT and in South Africa.

Recently Boksenberg, in collaboration with several European astronomers, mostly of ESO, applied for and obtained observing time on the ESO 3.6-m telescope at La Silla. He brought his instrument to La Silla first in August 1978, then in May 1979, and he has a run scheduled for March 1980. The ESO runs with the IPCS are two weeks long so as to make it worth while installing the instrument on the telescope, and are shared by about half a dozen astronomers. Keith Shortridge and John Fordham, both of UCL, also come to La Silla to operate the system with Boksenberg.

### 2.1

The image intensifier is a 4-stage EMI tube which is magnetically focused and operates at 45 kV. Its face-plate is highly transparent down to the atmospheric cut-off at 3000 Å. The tube is usually used with an S-20 photocathode, allowing one to observe up to 8500 Å. The quantum efficiency of the photocathode is 10% and the over-all blue-light gain of the tube is  $10^7$ , i.e.  $10^8$  photons are generated at the phosphor screen for each photoelectron produced by the photocathode. The useful linear field at the entrance of the image intensifier is 35 mm.

The television camera is a Philips Plumbicon, which is a standard camera tube for colour television; the photosensitive layer is a polycrystalline lead-oxide layer which is formed structureless. Its sensitivity is about 70% and it is peaked in the blue to match the P-11 phosphor screen of the image intensifier.

There is a transfer lens coupling the phosphor screen of the image intensifier and the entrance face of the television tube. This F/2 lens is optimized in the blue and transfers 1% of the photons. Thus for each primary photoelectron there are  $7 \times 10^5$  electrons in the television camera target. This gives a good video signal for further processing. (See figure 1.)

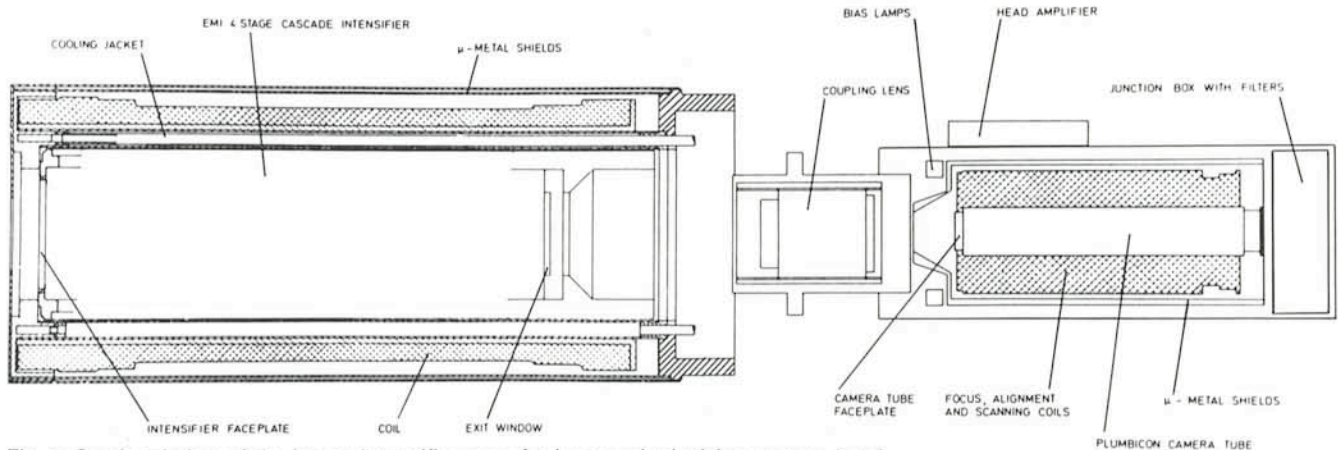


Fig. 1: Sectional view of the image intensifier, transfer lens, and television camera head.



## Proceedings of the ESO Workshop on Two Dimensional Photometry Soon Available

The Proceedings of this workshop have now been edited and will be available in print at the end of April 1980.

The price for the 412-page volume is Swiss Francs 40.— including postage. Please send your order to:

European Southern Observatory  
c/o CERN  
Attn. Miss M. Carvalho  
CH-1211 Geneva 23

### 2.2

In the format used at La Silla, the camera scanned 1,532 lines of 113 pixels each, and the "data window" (the area from which data were recorded) was 1,500 by 72. The frame is read perpendicular to the wavelength dispersion, i.e. one scan-line corresponds to one wavelength.

Photon and ion events are of a substantial size, covering up to 5 and 9 lines, respectively, for the 1,532 by 113 format. On passing through the shift register array these data are analysed by a hard-wired pattern recognition system, and the centre of the event, in the direction perpendicular to the scan-line, is determined. This position is then transferred to the computer system for incrementing the associated memory location, there being one location for each pixel within the "data window". Ion events are rejected in the pattern recognition system by comparing data in the photon + ion shift registers with those in the ions-only shift registers.

The number of photons per pixel per second beyond which saturation occurs depends on the speed with which the frame is read. With the large format used during the observations at La Silla, 1,532 lines of 113 pixels each, saturation starts at a rate of photon arrival in excess of one photon per pixel per second.

In practice, saturation is seldom a problem since the instrument is used to observe extremely faint stellar objects or extended objects of faint surface brightness. But care must be exercised in the choice and the observations of standard stars.

### 3. Data Acquisition and Data Reduction

The IPCS was installed on the 140-mm camera of the Boller and Chivens spectrograph at the Cassegrain focus of the 3.6-m telescope. As stated in section 2.2, the data window is 72 x 1,500, i.e. one IPCS image or frame is formed by 72 spectra of 1,500 pixels each. The distance between the individual spectra is 1"7 and the whole image covers 2'. With the 600 lpm grating, the wavelength range covered is 4320 Å, corresponding to 2.28 Å per pixel.

An image of the He-Argon comparison spectrum is taken for each galaxy or star image, and when observing galaxies which extend over the whole slit length, images of the blank sky are also taken to enable sky subtraction to be performed. As usual, the pixel-to-pixel variations are calibrated by taking an image of a flat field, and the response curve versus wavelength is determined by observing standard stars.

At ESO in Geneva, there are two ways of doing the dispersion correction of the images. One way is to consider each of the 72 spectra individually and to reduce them separately as if, for example, they were IDS scans. A batch command allows automatic reduction of all the individual spectra in a frame after the first one has been reduced.

The main shortcoming of this method is that it does not use all the information contained in the arc images; specifically, it does not use the fact that each line of the comparison arc is continuous and can be represented by a smooth function such as a polynomial. Dr. Werner Krischer at CERN has developed a powerful computer programme to extract the shape of particle tracks recorded on bubble chamber photographs. This programme is being adapted to the reduction of IPCS spectra by Cheryl Bettels of ESO with the help of Dr. Krischer and Dr. Danziger.

### 4. Results on Elliptical Galaxies

#### 4.1 Scientific Rationale

It has been known for several decades that a small fraction of elliptical galaxies contain some ionized gas.

Basic information such as the spatial distribution, the angular momentum, and the total mass of the interstellar gas in ellipticals is essentially missing. Even the origin of the gas is uncertain.

The amount of gas now observed in elliptical galaxies is much smaller than the quantity of gas produced by the stars through their evolution. There must, therefore, be an effective mechanism removing most of the gas from the ellipticals. Moreover, there is a large dispersion in  $M_{\text{gas}}/M_{\text{total}}$  among ellipticals. Could this be caused by an irregular rate of gas production? or is it due to irregularities in the regime of galactic winds believed to sweep ellipticals of most of their interstellar gas? An alternative explanation for the dispersion in  $M_{\text{gas}}/M_{\text{total}}$  is that some ellipticals are accreting intergalactic gas, as suggested by the recent discovery that a number of ellipticals have large irregular-shaped clouds of neutral hydrogen. If this later explanation turns out to be correct then the usual assumption, that galaxies do not receive any new material after the epoch of galaxy formation, should be abandoned.

A second important question relative to the interstellar gas in elliptical galaxies is the relationship between the interstellar gas and the radio galaxy phenomenon. It has recently become evident that many radio galaxies exhibit extended (i.e. extra-nuclear) optical emission features. In some cases, studies of long slit spectrograms have led astronomers to suggest that such features are "jets" of material, related in some unspecified way to the radio features or optical continuum jets being shot out from the galaxies' nuclei. A study by Ford and Butcher (*Ap.J.* 1979, in press) of the emission in M87, however, led those astronomers to conclude that the features in that galaxy are most likely manifestations of matter *infall* into the nucleus.

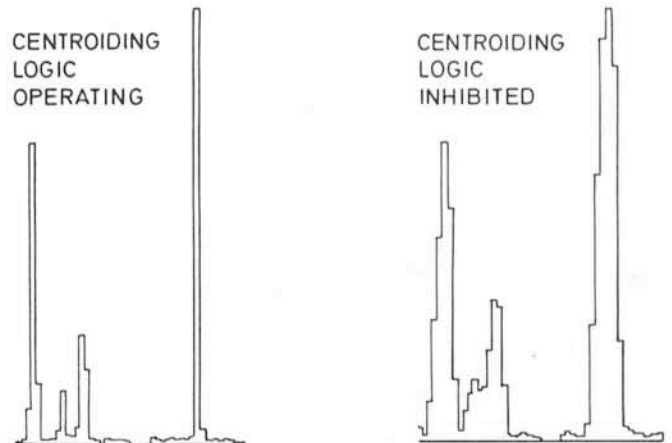


Fig. 2: Comparison lines. The centroided line-spread-function is less than one channel wide, while the non-centroided case extends over many channels.



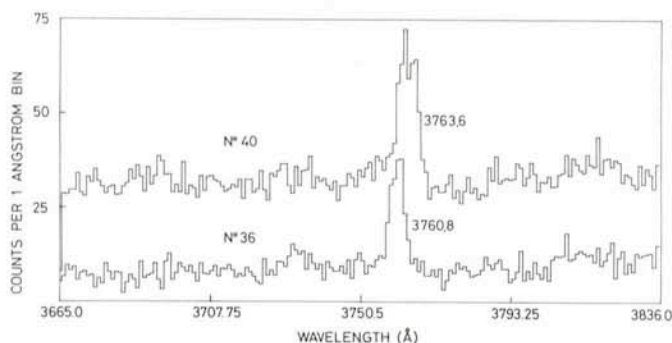


Fig. 3: Two individual spectra extracted from an image of the spectrum of the elliptical galaxy NGC 3962. The two spectra come from two points symmetrically located with respect to the nucleus and distant by 900 pc from the nucleus. The measured wavelengths of the  $[OII]\lambda 3727$  indicate velocities of 2895 and 2670  $\text{km s}^{-1}$ .

If this is the case, then the presence of the gas is likely to be one of the elements leading to the formation of the radio source rather than a consequence of the radio source phenomenon. It is not possible to reach a definitive conclusion on this important question because detailed data on the gas exist only for a few exceptional ellipticals which have been studied because they are powerful radio sources, and quantitative information on normal ellipticals which could be used for comparison is lacking.

For the reasons just outlined above, a fairly extensive spectrographic survey of elliptical galaxies with reported nuclear or extended emission seems to be called for. I engaged in such a survey in the spring of 1979 with the following aims: (i) to map the distribution of the ionized gas; (ii) to measure the velocity field; (iii) to measure the absolute line intensities and line intensity ratios.

#### 4.2 Results

The mapping of the gas was done in the spring of 1979 in collaboration with Harvey Butcher. We used the video cam-

era system on the KPNO 4-m telescope to make direct imagery of a number of elliptical galaxies through narrow-band filters centred on the red-shifted  $H\alpha + NII \lambda 6584$  lines and on an adjacent continuum band. In May 1979 the velocity field of a few of these galaxies was measured in a subsequent observing run with the IPCS at La Silla. The conclusion which can be drawn is that the gas shows velocity gradients of up to 200  $\text{km s}^{-1}$  over a distance of 1 to 4 kpc, and evidently does not partake in the motions of the stars. The data on the velocity field are now being interpreted and detailed results will be presented later.

Figure 3 shows an example of the data obtained with the IPCS. It is extracted from an image of the spectrum of the elliptical galaxy NGC 3962. The two individual spectra, No. 36 and No. 40, come from two points that are symmetrically located with respect to the nucleus, and are distant by 3.4 or 900 pc from the nucleus. The velocities measured by fitting the  $[OII]\lambda 3727$  unresolved doublet by a Gaussian profile are 2895 and 2670  $\text{km/s}$ , respectively. This assumes that the doublet ratio, which is density-sensitive, is the same in the two regions sampled by these spectra; this assumption has been verified by taking spectra in the  $H\alpha$ ,  $[NII]\lambda 6548$ , 6584 region.

Another example of what can be achieved with the IPCS is illustrated in figure 4.

Figure 4 is extracted from an IPCS frame taken with the spectrograph slit located at 5" or 9 kpc from the nucleus of 3C 445, which is a powerful radio galaxy with a Seyfert-type nucleus. Figure 4 shows the added signal coming from four contiguous spectra, which altogether cover the whole extent of the nebulosity in the EW direction, i.e. 6"8 (thick line). The thin line is the scaled average of the sky spectrum obtained from 40 individual spectra containing sky signals only.

Figure 5 shows the spectrum of the nebulosity and of the nucleus after sky subtraction and photometric calibration.

Differences in line intensity ratios and line width between the nucleus and the nebulosity are evident. The line inten-

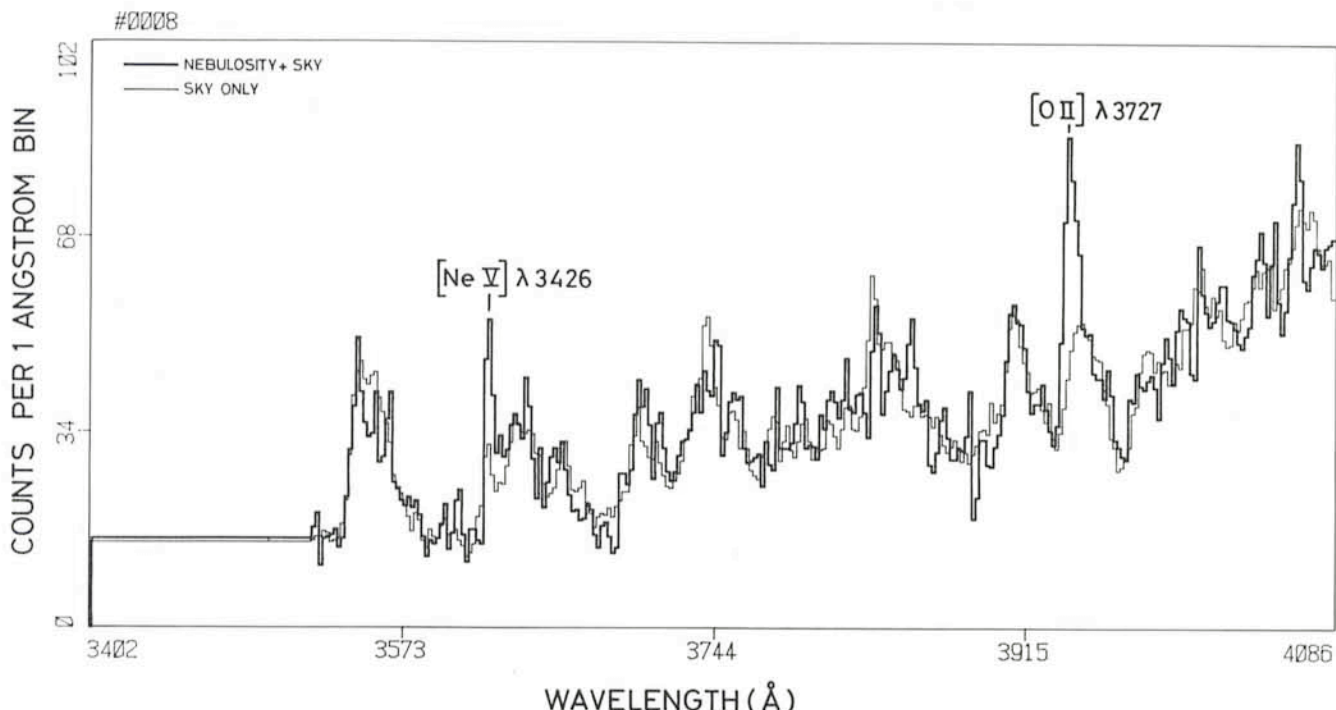


Fig. 4: Portion of the spectrum of the gaseous nebulosity observed at 9 kpc from the nucleus of 3C 445. The thick line is the sum of the signal from 4 contiguous spectra covering the whole nebulosity in the EW direction. The thin line is the scaled average of the sky spectrum obtained from adding 40 spectra containing sky signal only.

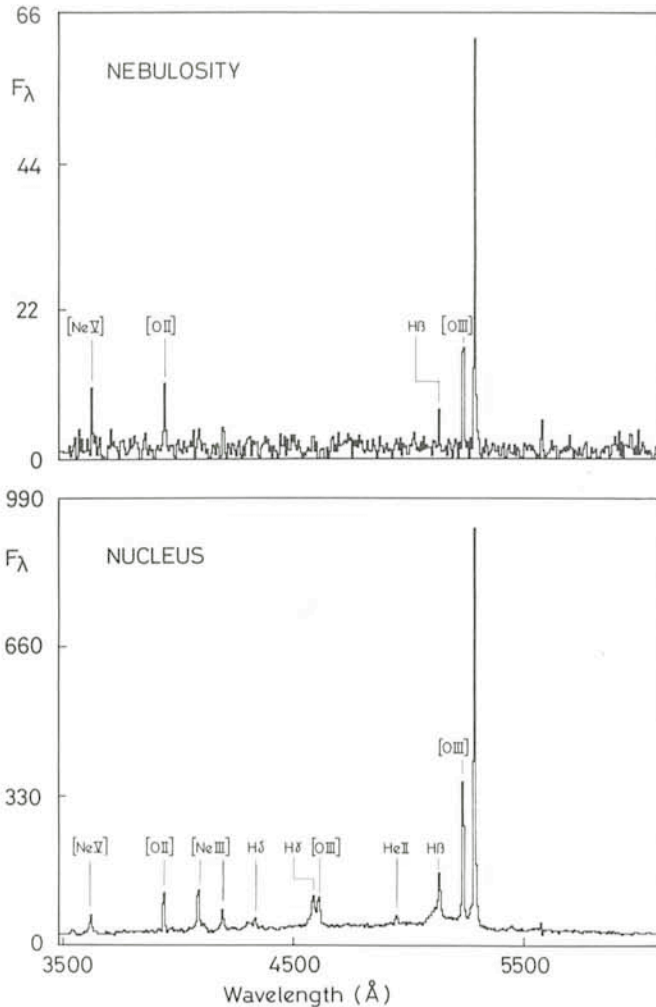


Fig. 5: Spectrum of the nebulosity and of the nucleus of 3C 445 after sky subtraction and photometric correction.

sities in the nucleus indicate a wider range of ionization than in the nebulosity. The interpretation of the spectrum of the nebulosity has been done as follows: in a nebulosity exposed to an ionizing source located at a distance  $R$ , the degree of ionization and therefore the line intensity ratios are essentially set by the parameter  $\varphi/n_{\text{part}}$ , which is the ratio of

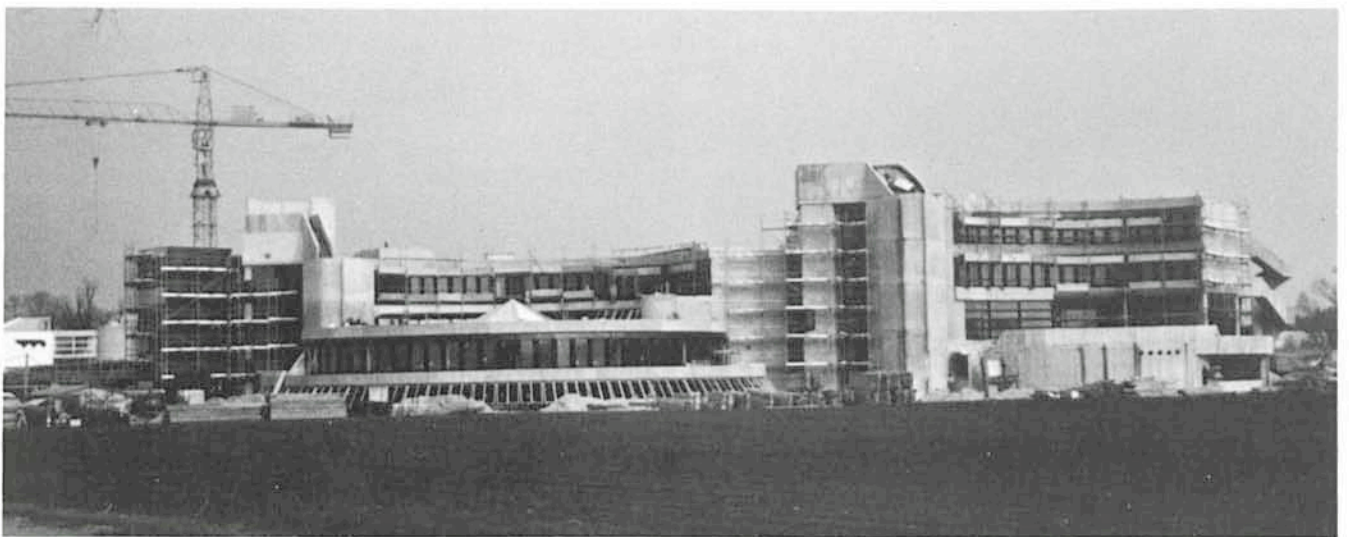
the ionizing flux incident on the nebulosity to the density of particles in the nebulosity;  $\varphi$  is equal to  $L_V/4\pi R^2 h_\nu$ , where  $L_V$  is the absolute luminosity of the ionizing source. If  $\varphi$  is known, then the line intensity ratios give the particle density. Daniel Pequignot of Meudon Observatory and I have recently calculated models for a nebulosity exposed to a power-law ionizing spectrum and have applied them to the highly ionized nebulosity associated with the SB0 Seyfert galaxy NGC 3516 (Ulrich and Pequignot, 1 May, 1980, *Astrophysical Journal*, in press). These models can be applied to 3C 445. In this case,  $L_V$  is estimated from the value of the continuum intensity of the nucleus at 3300 Å and assuming that the ionizing spectrum is a power law  $f_\nu \propto \nu^{-1}$ . Projection effects are neglected and  $R$  is taken to be equal to 9 kpc. For the value of  $\varphi$  so calculated, the line intensity ratios in the nebulosity of 3C 445 correspond to  $n_{\text{part}} \sim 15 \text{ cm}^{-3}$ . This gives a total mass for the nebulosity observed in an area of  $6''.8 \times 1''.7$  ( $11 \times 2.8 \text{ kpc}$ ) of  $10^6 M_\odot$ , i.e. as large as the mass of ionized gas present in the nucleus.

There are a number of cases already known of ionized nebulosities associated with quasars and radio galaxies and located at large distances from the nucleus. This is, however, the first case where the density of the nebulosity is determined. The reason is that we could detect [Ne V]  $\lambda$  3426, which is a good diagnostic of the degree of ionization. This detection was made possible by using a sensitive digital detector, which enabled us to detect faint lines and to perform sky subtraction satisfactorily.

## ESO Headquarters Building Nearing Completion

In spite of the winter, construction work on the ESO Headquarters building has rapidly advanced during the past months. The outside is almost terminated and the work is now concentrating on the technical installations inside the building.

Below and on page 12 we show some photographs of the building, all taken on March 24.



ESO European Headquarters at Garching. View taken from the rear of the building (south-west). / La sede principal de la ESO. Vista de la parte posterior del edificio (lado sudoeste).